Original Article | Journal of Biosystems Engineering

J. of Biosystems Eng. 39(3):205-214. (2014. 9)
http://dx.doi.org/10.5307/JBE.2014.39.3.205

eISSN : 2234-1862
pISSN : 1738-1266

Monte Carlo Simulation of Phytosanitary Irradiation Treatment for Mangosteen Using MRI-based Geometry

Se-Yeol Oh, Jongsoon Kim*, Soon-Hong Kwon, Sung-Won Chung, Soon-Goo Kwon, Jong-Min Park, Won-Sik Choi

Department of Bio-industrial Machinery Engineering, Pusan National University, Busan, Korea

Received: August 5th 2014; Revised: August 21st 2014; Accepted: August 22nd 2014

Abstract

Purpose: Phytosanitary irradiation treatment can effectively control regulated pests while maintaining produce quality. The objective of this study was to establish the best irradiation treatment for mangosteen, a popular tropical fruit, using a Monte Carlo simulation. **Methods:** Magnetic resonance image (MRI) data were used to generate a 3-D geometry to simulate dose distributions in a mangosteen using a radiation transport code (MCNP5). Microsoft Excel with visual basic application (VBA) was used to divide the image data into seed, flesh, and rind. Radiation energies used for the simulation were 10 MeV (high-energy) and 1.35 MeV (low-energy) for the electron beam, 5 MeV for X-rays, and 1.25 MeV for gamma rays from Co-60. **Results:** At 5 MeV X-rays and 1.25 MeV gamma rays, all areas (seeds, flesh, and rind) were irradiated ranging from 0.3 ~ 0.7 kGy. The average doses decreased as the number of fruit increased. For a 10 MeV electron beam, the dose distribution was biased: the dose for the rind where the electrons entered was 0.45 ± 0.03 kGy and the other side was 0.24 ± 0.10 kGy. Use of an electron kinetic energy absorber improved the dose distribution in mangosteens. For the 1.35 MeV electron beam, the dose was shown only in the rind on the irradiated side; no significant dose was found in the flesh or seeds. One rotation of the fruit while in front of the beam improved the dose distribution around the entire rind. **Conclusion:** These results are invaluable for determining the ideal irradiation conditions for phytosanitary irradiation treatment of tropical fruit.

Keywords: Mangosteen, Monte Carlo, MRI, Phytosanitary irradiation

Introduction

Mangosteen is a tropical fruit that is mainly grown in Southeast Asia. The fruit is spherical and its diameter is about 5 cm. The edible flesh is composed of 4 to 8 segments contained in an 8 to 10 mm thick rind. The production volume of mangosteen is increasing and it is now being processed into value-added products such as jam, candy, and wine. In addition, the fruit pericarp (rind) can be used as an anti-bacterial agent and for curing diarrhea (Diczbalis, 2011). Thailand, the world's largest producer of mangosteen, grows approximately 46,000 metric tons (MT) annually (Osman, 2006).

***Corresponding author:** Jongsoon Kim
Tel: +82-55-350-5426; **Fax:** +82-55-350-5429
E-mail: jongsoon-kim@pusan.ac.kr

Good quarantine processes save economic and social resources. The losses caused by plant pests and diseases is anywhere from 20 to 40 percent of global crop yields (FAO, 2012). There are a few methods of phytosanitary treatment used commercially: hot water treatment, cold treatment, irradiation, fumigation, and hot air treatment. For the hot water treatment, mango is immersed into hot water at 46°C for 65 to 110 minutes to get rid of fruit flies (Mitcham and Yahia, 2008). The problem with this treatment is the loss of quality. A cold treatment requires storing the commodity at a little above freezing temperature for a reasonable period of time (Gould, 1994). Fumigation uses chemicals in a gas state to penetrate into hole or crack of the outer skin of fruits (Bond, 1984). Methyl bromide, a toxic chemical, has been widely used in fumigation. Methyl bromide fumigation has been permitted for mangosteen

imported to Australia from Thailand or Indonesia. However, deaths and injuries have been associated with use of this material (Anon, 1994). Hot air treatment involves blowing heated air through stacks of fruit. The air supply is set for specific temperatures, relative humidity, and duration, depending on the commodity and the pests (Hallman and Armstrong, 1994). Like hot water treatment, hot air treatment causes commodity quality problems. However, irradiation treatment is safe for human and animals, because unlike chemical treatment, it does not leave a residue. Irradiation also achieves its effects without significantly raising the temperature of the food, leaving it closer to its unprocessed state.

Irradiation uses the energy of electron beams, X-rays, and/or gamma rays to break the chemical bonds of organisms like insects or eggs at a reasonable depth of fruit. The main issue with irradiation is to treat the target uniformly in a cost-efficient way. Irradiation treatment is very effective for pest control, compared with other treatment methods. It can be even applied to commodities that are already packed. Currently, irradiation treatment is performed in six countries for quarantine purposes and the annual amount of tropical fruit processed is 19,000 tons (Hallman, 2011). The mangosteens imported to the USA from Thailand are irradiated with a minimum dose of 400 Gy for phytosanitary purposes (Tunlayadechanont, 2013).

Commercial irradiation treatment facilities use gamma rays from Cobalt-60, or X-rays or electron beams that are machine generated. The amount of the absorbed energy is called a dose, and the unit is a gray (Gy); one Gy is 1 joule of energy absorbed in 1 kg of substance. Dose uniformity ratio (DUR) is the ratio of the maximum dose to minimum dose over the irradiated target. However, it is not easy to figure out which part of the object gets how much irradiation, because of the dosimeter's geometric limitations. Sometimes fruits are not rigid enough to bear the process of dose measurement. Furthermore, it is almost impossible to obtain whole dose distribution in the sample with the discrete use of dosimeters. Thus, a simulation technique is required to better understand the dose distribution in samples.

The Monte Carlo method is a computational algorithm in which we can obtain numerical results from repeated random sampling. It is mostly used in physics or mathematics-related engineering problems (Elishakoff, 2011). The modern version of the Monte Carlo method was invented in the late 1940s by Stanislaw Ulam while he was working on nuclear weapons projects at the Los Alamos National Laboratory of Department of Energy in USA. John Von Neumann understood its importance and programmed the ENIAC computer to carry out Monte Carlo calculations (Anderson, 1986). This Monte Carlo N-Particle Transport Code (MCNP) developed for simulating nuclear processes has had several improvements. The Monte Carlo method also has been used in agriculture: soil mapping (Fisher, 1991), herbicide application (Matsui et al., 2005), and microbial risk assessment model (Puerta-Gomez et al., 2013).

Magnetic resonance imaging (MRI) is a medical imaging technique used to visualize the internal structures of the body in detail. Even though computed tomography (CT) data has been used for radiation simulation for heterogeneous complex-shaped foods (Borsa et al., 2002; Kim et al., 2006b), MRI can provide better contrast between the soft internal parts of foods, because CT data are strongly dependent on density. Thus, geometric information for accurate dose calculation in a Monte Carlo simulation can be obtained with multi-sliced MRI data. In food research, MRI has been applied for structure measurement (Musse et al., 2014), moisture and lipid distributions (Chen et al., 2010; Rumsey and McCarthy, 2012), and phase transitions (Lucas et al., 2005). However, no literature is available regarding MRI application to phytosanitary irradiation treatment.

The main goal of this study was to obtain the dose distribution in mangosteen using Monte Carlo simulation and MRI data and then establish the proper irradiation treatment for phytosanitary purpose.

Materials and Methods

MRI measurements

Mangosteens in a frozen state were purchased from a local grocery store and stored at -10°C before the experiment. MRI measurements were carried out using a 4.7T BioSpec 47/40 scanner (Bruker, Woodland, TX, USA) installed at the Korea Basic Science Institute (KBSI, Osong, Korea). A multi-slice multi-echo (MSME) sequence was used to acquire images with a 10.0 ms echo time and a 600 ms repetition time (T1-weighted scan, Figure 1(a)). A rapid acquisition with relaxation enhancement (RARE) sequence was also used to acquire images with a 90.0 ms echo time and a 6,000 ms repetition time (T2-weighted scan, Figure

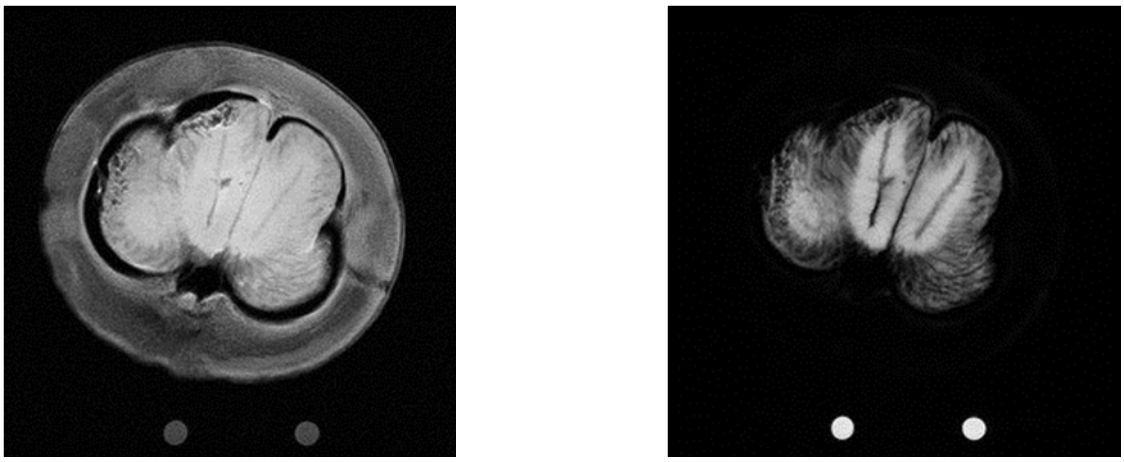

(a) (b)

Figure 1. MR image of mangosteen in (a) T1-weighted scan and (b) T2-weighted scan.

1(b)). The field of view (FOV) was 60 mm; 25 images in the vertical plane were acquired, each with a slice thickness of 2 mm.

A T1-weighted scan provided appreciable contrast between the components of mangosteen (rind, flesh, and seed). A T2-weighted scan the rind was dark, due to lack of water.

The original MRI data in DICOM (Digital Communications in Medicine) format were converted into text format image files using Image J software (NIH, Bethesda, MD, USA, http://rsb.info.nih.gov/ij/). Those files consisted of a matrix of 256 x 256 pixels for segmentation and indexing.

Image processing with an excel macro

An Excel macro using VBA was used to process MRI data, instead of commercial image processing software, because Excel provides this application and data extracted from the images are easy to create, store, and use.

For the T1-weighted scan, the boundary between rind and air had a distinct intensity level; thus, edge detection technique was used to segment the rind area. Figure 2 shows the intensity level histogram of flesh and seed for a T2-weighted scan. Note that the histogram is clearly bimodal, indicating the presence of the boundary between flesh and seed. Consequently, the seed region was easily isolated from the flesh region by placing a single threshold value (17,000) in the histogram valley. The mangosteen components, segmented and indexed, are shown in Figure 3, which was processed by a visualization macro.

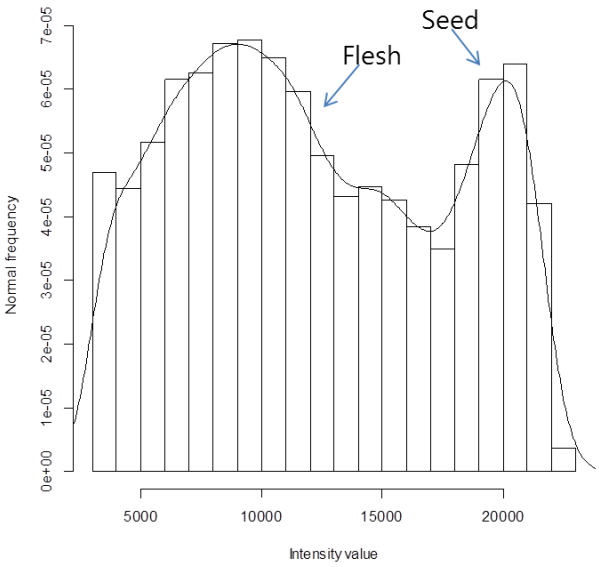

Figure 2. Intensity level histogram of flesh and seed at T2-weighted scan.

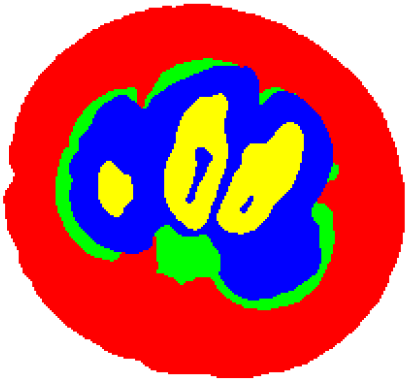

Figure 3. Mangosteen after segmentation using Excel Macro: rind (red), flesh (blue), seed (yellow), and air (green).

Monte Carlo simulation

The MCNP5 (Monte Carlo N-Particle, version 5), one of the most powerful simulation programs for high energy particle transport, along with EGS4 and GEANT4, was used to obtain the dose distribution in mangosteens. Electron Gamma Shower (EGS) (Nelson et al., 1985) and Geometry And Tracking (GEANT) (Agostinelli et al., 2003) are general purpose packages for the Monte Carlo simulation of the coupled transport of electrons and photons in an arbitrary geometry for particles with energies from a few KeV up to several TeV.

Three principle types of radiation sources can be used in food irradiation according to the Codex Alimentarius General Standard (FAO/WHO, 1984): gamma irradiation (1.25 MeV) from ^{60}Co radionuclides, machine sources of electron beams with energies up to 10 MeV, and machine sources of X-rays with energies up to 5 MeV. Recently, low-energy (1.35 MeV) electron beams were also used for surface irradiation of complex-shaped foods (Kim et al., 2006b). Thus, The radiation sources in the simulation were 5 MeV X-rays, 1.25 MeV gamma rays, and high-energy (10 MeV) and low-energy (1.35 MeV) electron beams.

The photons (X-rays and gamma rays) used in food irradiation penetrate a substantial thickness of solid material, enabling the treatment of pallet loads of commodities. Penetration by electron beam is much less than by photons and can only be used to treat produce loads of no more than 5-10 cm in depth, such as single layer of fruits or shallow boxes of cut flowers. In the simulation, each source particle was emitted in a plane, distributed evenly, and entered the target perpendicularly.

The repeated structure algorithm was used to construct the voxel of the mangosteen, and the geometry data arrays consisted of 11 x 109 x 109 voxels of 0.20 x 0.05 x 0.05 cm^3. Among 25 images, eleven slices were selected for actual simulation, considering the computing time. The nutrient values of flesh, seed, and rind were taken from the USDA National Nutrient Database, Ajayi et al. (2007), and Zadernowski et al. (2009), respectively. Those data were used to calculate their atomic compositions based on the elemental composition ratio in tissue (ICRP, 1975). Densities of the components were calculated by using the equation developed by Choi and Okos (1986). Table 1 shows the atomic composition and density of each component of mangosteen; C, H, O, N represents carbon, hydrogen, oxygen, and nitrogen, respectively. Since the flesh has high moisture content (80.94%), the weight fraction of oxygen is relatively higher.

The pulse height tally (F8) was used for scoring absorbed energy in a voxel. This tally scores the energy (MeV) of a photon or electron as it enters or leaves a cell, which is analogous to a physical detector. A positive energy tally occurs from particles entering a cell and a negative energy tally occurs from particles exiting a cell. The simulation was run on a Windows PC (3.20 GHz CPU, 32.0 GB RAM) with the Cygwin platform. The CPU time was approximately 9 hours or 10^6 histories. Monte Carlo simulation results represent an average of the contributions from many simulation histories. When the statistical uncertainty (relative error) is less than 5%, the simulation result then is reliable (Brown, 2003). Thus, each simulation history was varied to meet this guideline; there were approximately 10^6– 10^7 histories.

Table 1. The elemental composition (percent by mass) and density of mangosteen components (flesh, seed, and rind)

	C	H	O	N	Others (mineral)	Density (g/cm^3)
Flesh[a]	8.04	9.91	80.84	0.06	1.15	1.06
Seed[b]	43.73	7.87	43.69	1.05	3.66	1.23
Rind[c]	31.39	7.63	59.03	0.28	1.67	1.04

[a]Source: USDA National Nutrient Database for Standard Reference (Mangosteen, NDB NO: 09177).
[b]Source: Ajayi et al. (2007)
[c]Source: Zadernowski et al. (2009)

Results and Discussion

Dose distribution in mangosteen with 1.25 MeV gamma rays

Gamma rays from radioactive nuclides (^{60}Co) have been used as a suitable source of ionizing energy for irradiation treatment because of its greater penetrating capability. This radiation is essentially mono-energetic (1.25 MeV); ^{60}Co emits two photons per disintegration simultaneously, with energies of 1.17 MeV and 1.33 MeV.

In this study, the target dose was set to 0.4 kGy, which is the generic radiation dose endorsed by the USDA-APHIS. “Generic” refers to a treatment for a broad group of pests on all commodities. This dose is fully effective with less influence on the quality of most commodities (Hallman, 2011).

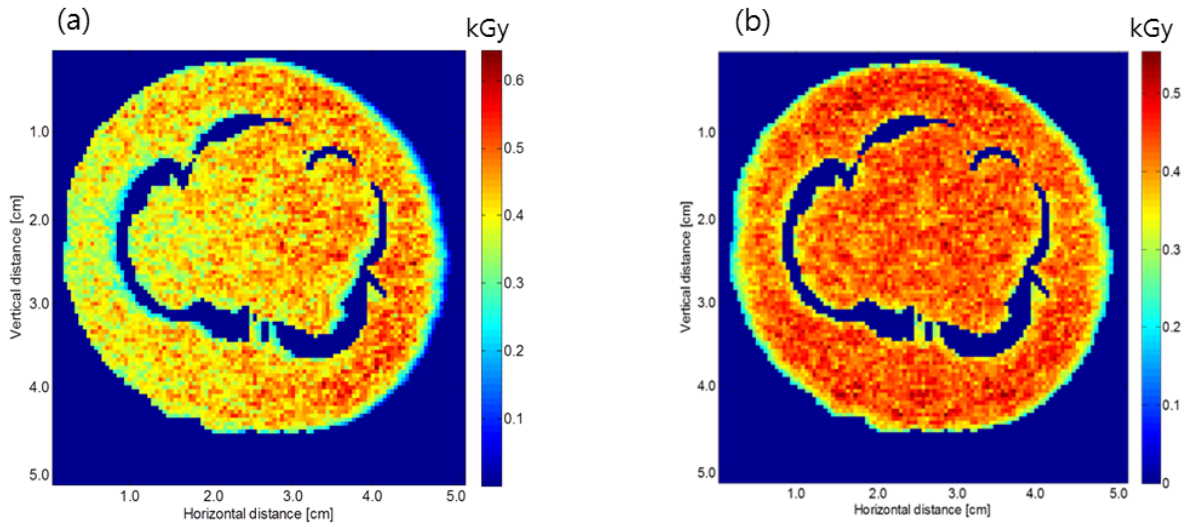

Figure 4. Dose distribution in mangosteen with 1.25 MeV gamma rays (a) in one-sided irradiation and (b) in two-sided irradiation.

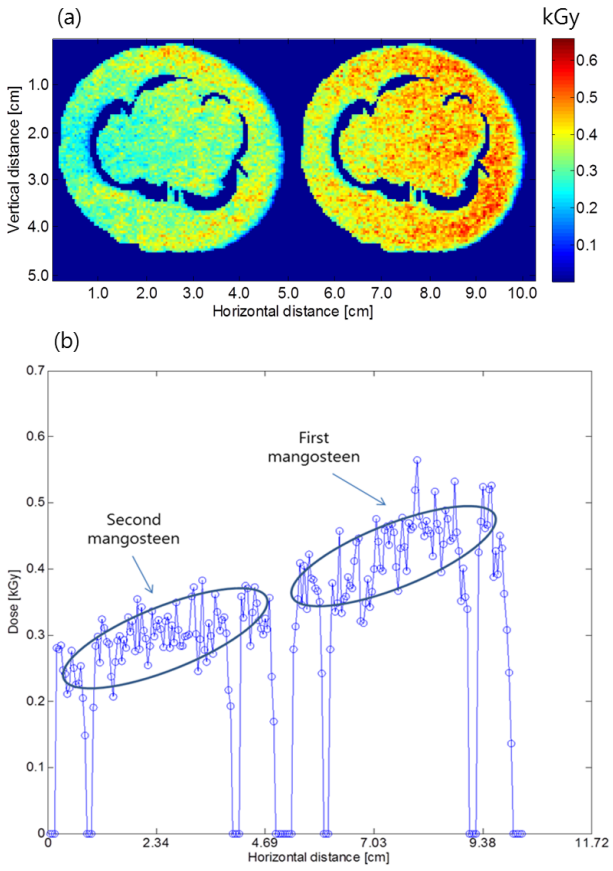

Figure 5. Dose distribution in mangosteen with 1.25 MeV gamma rays (a) in two mangosteens; (b) dose profile along the horizontal direction at a vertical point of 2.3 cm.

Figure 4(a) shows the dose distribution in mangosteen when the gamma rays flow toward the left. In general, gamma rays lose their kinetic energy in large interactions and have no limiting range through matter; thus, the absorbed dose was presented in the whole mangosteen.

In the one-sided irradiation, the portion of the rind under-irradiated (less than 0.3 kGy) was 9.6% of the total rind area. After the treatment, the living pests in that portion would increase their number rapidly, resulting in nullifying the irradiation effect. For the two-sided irradiation, the portion under-irradiated decreased to 8.5% and it was mainly located on the surface area (approximately 1 mm depth) of the rind where the pests are less likely to reside in (Figure 4(b)). The portion at the rind over irradiated (larger than 0.5 kGy) was decreased from 8.5% at the one-sided irradiation to 2.4% at the two-sided irradiation. However, the dose in the flesh was 0.41 ± 0.04kGy, which would be a concern for preserving the quality of the fruit.

In commercial applications, more than one fruit is exposed to the irradiation sources at a time (Figure 5(a)). The average doses of the rind in the first and second mangosteen were 0.40 ± 0.08 kGy and 0.33 ± 0.07 kGy, respectively. It turns out that the average dose decreases as the number of fruit increases (Figure 5(b)). Thus, just as for one mangosteen, two-sided irradiation should be applied to improve the dose distribution at multiple mangosteens.

Dose distribution in mangosteen with 5 MeV X-rays

X-rays are generated from electron accelerators. A 5 MeV electron beam (in this case) strikes a converter

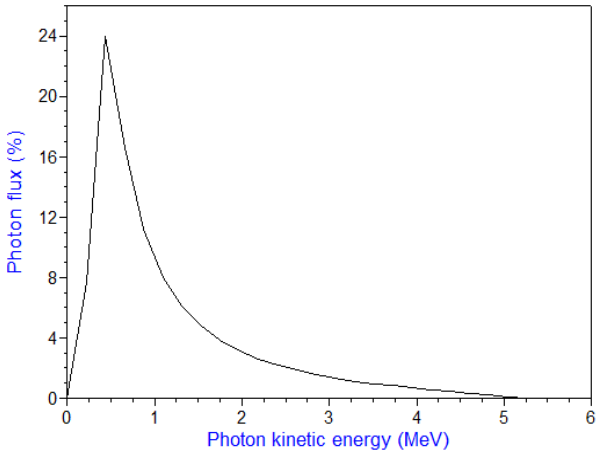

Figure 6. Photon energy spectrum from 5 MeV electrons (Kim et al., 2006a).

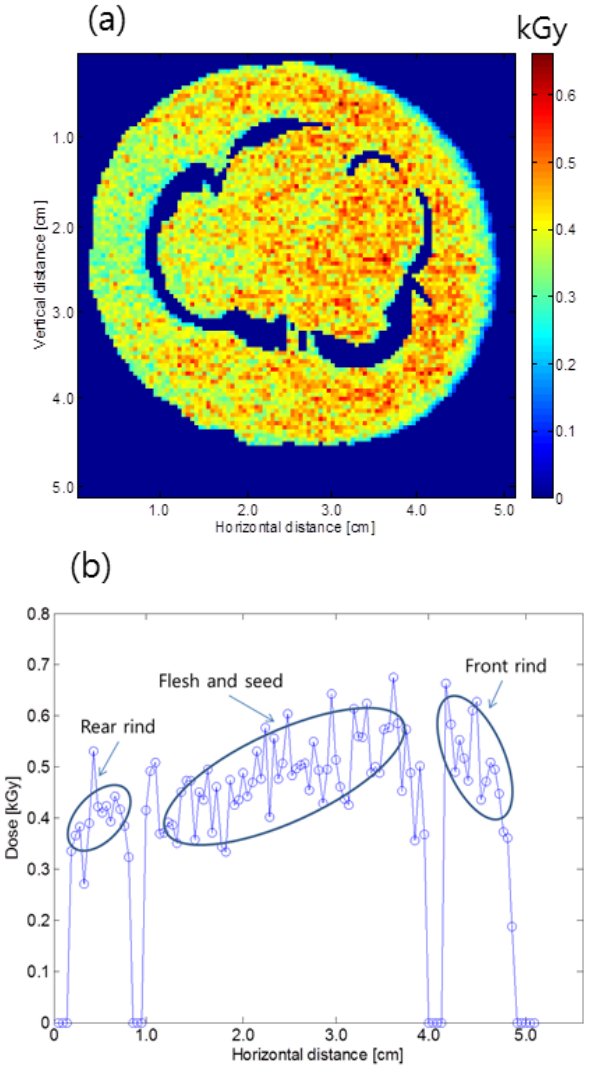

Figure 7. Dose distribution in mangosteen with 5 MeV X-rays (a) at the westward beam direction; (b) dose profile along the horizontal direction at a vertical point of 2.3 cm.

metal like tantalum (Ta), tungsten (W), or gold (Au), which generates X-rays in a target direction. In contrast to the radionuclide sources, which emit nearly mono-energetic photons, X-rays emit photons with a broad energy spectrum. Since the attenuation of photons is dependent on their energy, we must take into account the entire energy spectrum to calculate accurate dose distribution. The X-ray spectrum used in this simulation is shown in Figure 6 (Kim et al., 2006a); the average kinetic energy is 0.76 MeV, which is far less than the input energy (5 MeV).

Figure 7 shows the dose distribution result from the simulation. It is similar to the 1.25 MeV gamma ray simulation except it is a little higher at the front half. The dose is distributed over the whole mangosteen and it decreases as the X-rays proceed through the mangosteen (Figure 7(a)). Since the incident photon energy spectrum was broad, there was a long dose buildup depth: approximately 1.0 cm (Figure 7(b)). In fact, the buildup depth at 1.25 MeV gamma rays was 0.5 cm (Weiss and Rizzo, 1970). The dose decrease was also pseudo-exponential since the superposition of a series of exponential curves was not exactly exponential. Thus, in the X-ray irradiation, the lateral dose distribution is more uniform; however, it is less useful in the surface treatment.

Dose distribution in mangosteen with 10 MeV electron beam

Figure 8(a) shows the simulation result of mangosteen at 10 MeV electrons in the westward beam direction. The absorbed dose covered the whole mangosteen; however, the doses at the right half were much higher than the ones at the left half. The high dose region became narrower as the electrons moved from the center to the edge.

The dose distribution in the whole mangosteen was strongly related to the electron's incident angle. When the angle of incidence is greatly increased (away from normal), the electrons scatter more easily as they penetrate. Thus, the dose in the rind at the right half was 0.45 ± 0.03 kGy, whereas the dose in the rind at the left half was 0.24 ± 0.10 kGy (Figure 8(b)). For the two-side irradiation, the dose in the whole rind was significantly improved (0.34 ± 0.06 kGy) and the dose in the whole flesh (0.34 ± 0.03 kGy) was similar to the one in the rind.

Unlike the photons, which theoretically have no limiting range through matter, electrons have a distinct penetration depth because they interact with one or more electrons of practically every atom they pass. Thus, if we put a kinetic

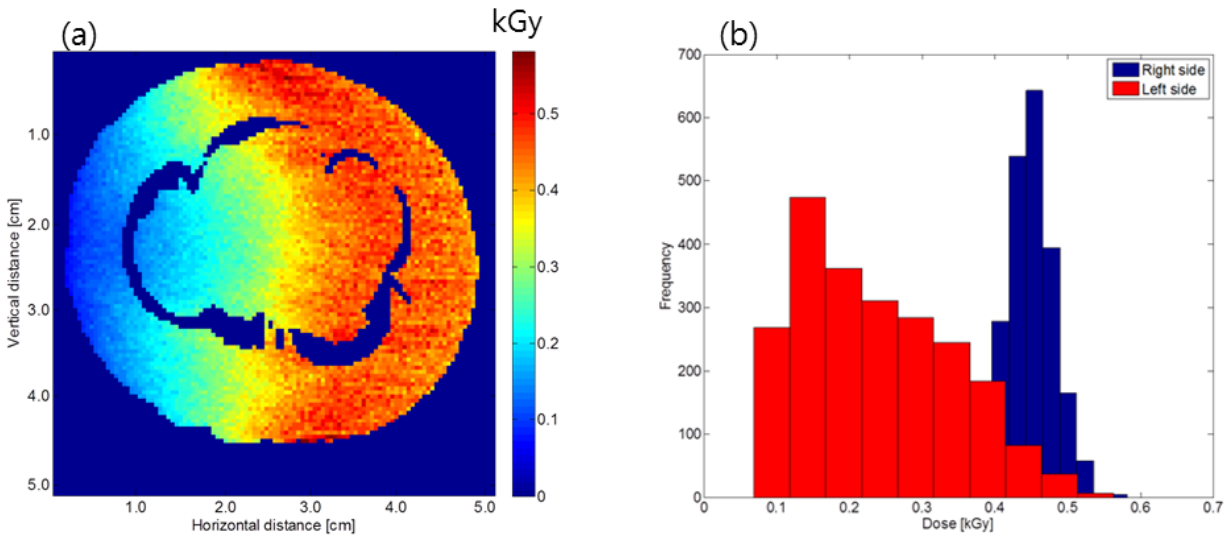

Figure 8. Dose distribution in mangosteen with a 10 MeV electron beam (a) in the westward beam direction (b) dose profile for the rind (red: the left side, blue: the right side).

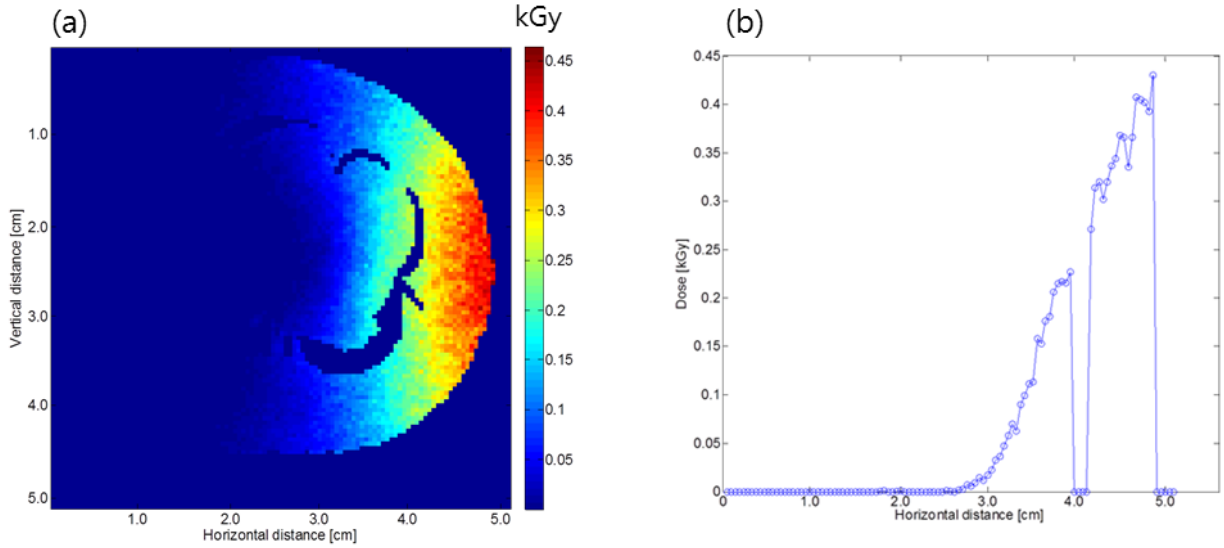

Figure 9. Dose distribution in mangosteen with a 3 cm thick Lucite block with a 10 MeV electron beam (a) in the westward beam direction (b) dose profile along the horizontal direction at the center at 2.3 cm.

energy absorber (e.g., plastic block) between the electron beam and the mangosteen, we can minimize the radiation effect to the flesh; the plastic block absorbs the incoming energy from the electron beam so the penetration depth is reduced.

Figure 9(a) shows the dose distribution in mangosteen with a 10 MeV electron beam with a 3 cm thickness of Lucite block (Polymethyl methacrylate (PMMA), $\rho = 1.18$ g/cm^3); the electrons that reached the mangosteen surface only penetrated 2.2 cm more (Figure 9(b)), which was much less than the normal penetration depth (approximately 4.5 cm) for the 10 MeV electron beam. Like the case without the Lucite block, the penetration depth decreased as the electrons moved from the center to the edge due to the scattering of electrons in the Lucite block. This problem can be solved by placing a half cylinder-shaped Lucite, instead of a uniform thickness box-shaped Lucite; at the both edges, the Lucite thickness is very thin so that the penetration depth at the mangosteen increases, and at the center it is vice versa. On the whole, the use of the Lucite absorber at 10 MeV electron beam would be very effective to irradiate a rind uniformly and to preserve the fruit quality.

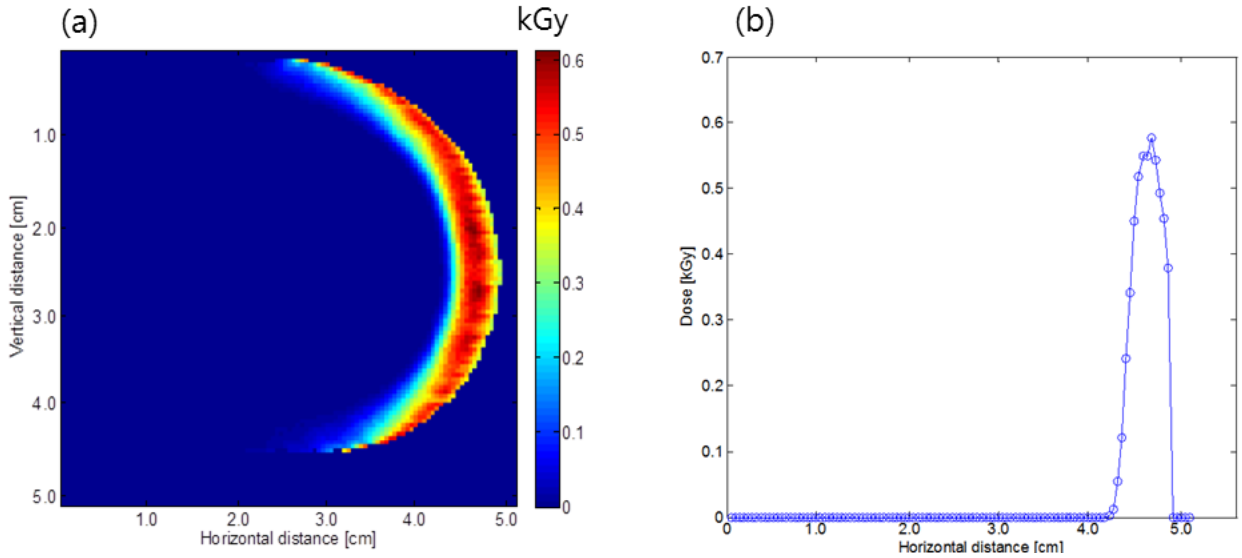

Figure 10. Dose distribution in mangosteen with a 1.35 MeV electron beam (a) in westward beam direction; (b) dose profile along the horizontal direction at vertical point of 2.3 cm.

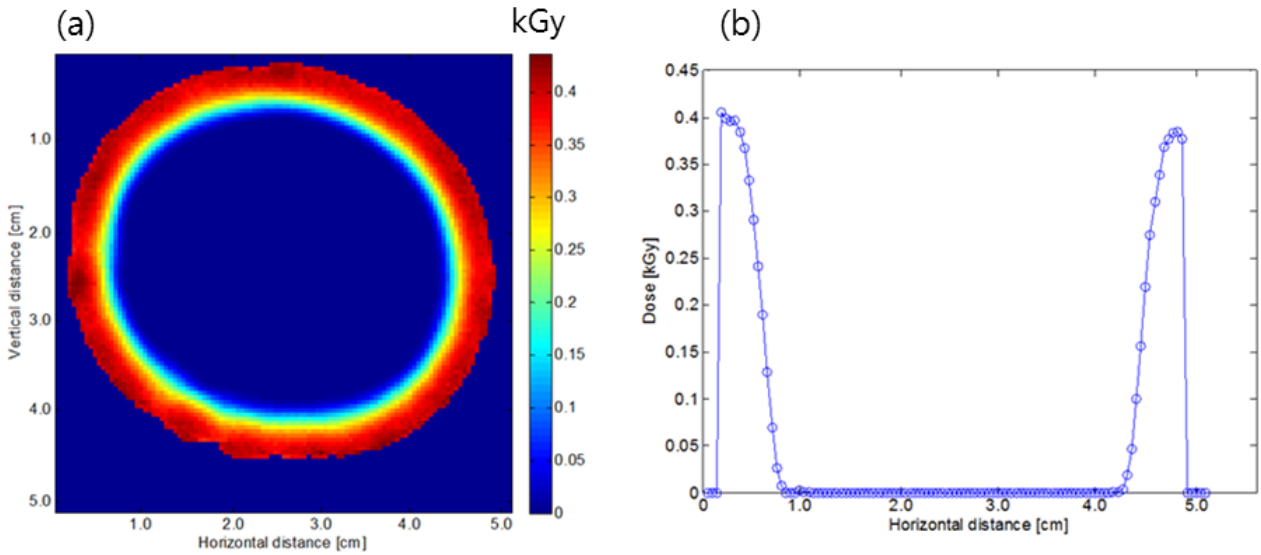

Figure 11. Dose distribution in mangosteen with a 1.35 MeV electron beam (a) in one whole rotation; (b) dose profile along the horizontal direction at a vertical point of 2.3 cm.

Dose distribution in mangosteen with a 1.35 MeV electron beam

The simulation result with the 1.35 MeV electron beam (Figure 10(a)) had two interesting features. One is that the dose was not shown after passing the rind (Figure 10(b)), e.g., in the edible flesh and seed. This is very promising, since the irradiation process with a 1.35 MeV electron beam does not affect the quality of the edible flesh. In fact, the absorbed dose was 52% higher at a 0.23 cm depth from the entrance and then rapidly fell until it went to zero. Its penetration depth was only 0.7 cm. The other is that the effective area of irradiation is biased to the direction of the beam source. The irradiation area was crescent-shaped, i.e., it was wider in the middle and pointed on the ends, and the area having at least 0.1 kGy was only 27% of the whole rind area.

Irradiation from two sides, obtained by turning the product, is often used to improve the dose distribution within the product. Even in two-sided irradiation, the doses and irradiation area at both ends of the mangosteen will be still lower. Therefore, unless the mangosteen rotates in front of the electron beam (Figure 11), this low-energy

(1.35 MeV) electron beam would not be adequate for phytosanitary irradiation treatment of mangosteen. In general, the electrons in the accelerator emerge into the air from a narrow window, and they are perpendicular to the flow motion of the conveyor. Thus, it is crucial to develop a method for rotating the sample on a conveyor without physical damage.

Conclusions

Because of the difficulty of measuring the dose inside a mangosteen, the only approach is to use a mathematical simulation. The Monte Carlo method is currently the most accurate procedure for dose calculations in electron beam and gamma/X-rays.

The simulation results from the 1.25 MeV gamma rays and 5 MeV X-rays showed similar dose distributions; the absorbed dose was presented on the whole mangosteen. When comparing irradiation treatment of mangosteen with 1.35 MeV to 10 MeV electron beam sources, the treatment with lower energy can more effectively control pests in the rind and preserve the quality than the higher energy treatment, which has a greater penetration depth. Therefore, when using high energy accelerators to treat the shallow region (e.g., rind) of fruits, careful planning is needed, since energy absorbers are required to reduce the entrance electron kinetic energy to the produce. This requires a fundamental understanding of electron beam interaction with the target produce.

The image source used in this study was MRI. Both T1-weighted and T2-weighted images were necessary for each slice to segment each part of the fruit. The tool used to process the image was Microsoft Excel.

Phytosanitary irradiation treatment is a promising quarantine process. Accurate dose calculation is required to establish practical processing facilities. The MR-image based Monte Carlo simulation approach could reduce the uncertainties associated with irradiation treatment; thus, the path is clear to realizing the full potential of irradiation as a phytosanitary treatment.

Conflict of Interests

The authors have no conflicting financial or other interests.

Acknowledgements

This work was partially supported by the Pusan National University Research Grant, 2011.

References

Anderson, H.L. 1986. Metropolis, Monte Carlo and the MANIAC. Los Alamos Science 14:96-108.

Agostinelli, S., J. Allision, K. Amako, J. Apostolakis, H. Araujo et al.,2003.GEANT4 – a simulation toolkit. Nuclear Instruments and Methods in Physics Research A, 506: 250-303.

Ajayi, I.A., R.A. Oderinde, B.O. Ogunkoya, A. Egunyomi, and V.O. Taiwo. 2007. Chemical analysis and preliminary toxicological evaluation of Garciniamangostana seeds and seed oil, Food Chemistry 101:999-1004.

Anon. 1994. Methyl bromide under fire. Environmental Health Perspectives 102, 732.

Bond, E.J. 1984. Manual of Fumigation for Insect Control. Rome: Food and Agriculture Organization of the United Nations.

Borsa, J., R. Chu, J. Sun, N. Linton and C. Hunter. 2002. Use of CT scans and treatment planning software for validation of the dose component of food irradiation protocols. Radiation Physics and Chemistry 63:271-275.

Chen, F.L., Y.M. Wei and B. Zhang. 2010. Characterization of water state and distribution in textured soybean protein using DSC and NMR. Journal of Food Engineering 100:522-526.

Choi, Y. and M.R. Okos. 1986. Thermal properties of liquid foods: Review. In *Physical and Chemical Properties of Food*, M.R. Okos (ed.) American society of Agricultural Engineers. St. Joseph, Mich., pp.35-77.

Diczbalis, Y. 2011 (revised). Farm and Forestry Production and Marketing Profile for Mangosteen (Garciniamangostana). In: Elevitch, C.R. (ed.). Specialty Crops for Pacific Island Agroforestry. Permanent Agriculture Resources (PAR), Holualoa, Hawai'i. http://agroforestry.net/scps

Elishakoff, I. 2001. Essay on the role of the Monte Carlo method in stochastic mechanics. In: *Monte Carlo Simulation*, eds. G.I. Schueller and P.D. Spanos, Abingdon: Balkema.

FAO. 2012. Available at: www.fao.org/news/story/en/item/131114/icode/

FAO/WHO. 1984. Codex General Standard for Irradiated

Foods and Recommended International Code of Practice for the Operation of Radiation Facilities used for the Treatment of Food, Codex Alimentarius. Rome, Italy.

Fisher, P.F. 1991. Modeling soil map-unit inclusion by Monte Carlo simulation. International Journal of Geographical Information Systems 5(2):193-208.

Gould. 1994. Cold storage. In: *Quarantine Treatment for Pests of Food Plants*, eds. J.L. Sharp and G.J. Hallman, Boulder, Colorado: Westview Press.

Hallman, G.J. 2011. Phytosanitary applications of irradiation. Comprehensive Reviews in Food Science and Food Safety 10:143-151.

Hallman, G.J. and J.W. Armstrong. 1994. Heated air treatments. In: *Quarantine Treatment for Pests of Food Plants*, eds. J.L. Sharp and G.J. Hallman, Boulder, Colorado: Westview Press.

ICRP. 1975. Report on the Task Group on Reference Man. ICRP Publication 23. Pergamon Press: International Commission on Radiological Protection.

Kim, J., R.G. Moreira, R. Rivadeneira, and M. E. Castell-Perez. 2006a. Monte Carlo-based food irradiation simulator. Journal of Food Process Engineering 29:72-88.

Kim, J., R.G. Rivadeneira, M.E. Castell-Perez and R.G. Moreira. 2006b. Development and validation of a methodology for dose calculation in electron beam irradiation of complex-shaped foods. Journal of Food Engineering 74:359-369.

Lucas, T., A. Grenier, S. Quellec, A.L. Bail and A. Davenel. 2005. MRI quantification of ice gradients in dough during freezing or thawing processes. Journal of Food Engineering 71:98-108.

Matsui, Y., T. Inoue, T. Matsushita, T. Yamada, M. Yamamoto, and Y. Sumigama. 2005. Effect of uncertainties in agricultural working schedules and Monte-Carlo evaluation of the model input in basin scale runoff model analysis of herbicide. Water Science Technology 51:329-337.

Mitcham, E., and E. Yahia. 2008. Alternative Treatments to Hot Water Immersion for Mango Fruit, *Report to the National Mango Board*.

Musse, M., S. Challois, D. Huc, S. Quellec and F. Mariette. 2014. MRI method for investigation of eye growth in semi-hard cheese. Journal of Food Engineering 121: 152-158.

Nelson, W.R., H. Hirayama and D.W.O. Rogers. 1985. The EGS4 code system. Stanford Linear Accelerator Center, Stanford, CA.

Osman, M. and M.A. Rahman. 2006. Mangosteen-Garciniamangostana. Southampton Centre for Underutilised Crops, University of Southampton, Southampton, UK.

Puerta-Gomez, A.F., J. Kim, R.G. Moreira, G.A. Klutke, and M.E. Castell-Perez. 2013. Quantitative assessment of the effectiveness of intervention steps to reduce the risk of contamination of ready-to-eat baby spinach with Salmonella. Food Control 31:410-418.

Rumsey, T.R and K.L. McCarthy. 2012. Modeling oil migration in two-layer chocolate-almond confectionery products. Journal of Food Engineering 111:149-155.

Tunlayadechanont, S. 2013. Fresh fruits irradiation for phytosanitary purposes in Thailand using a multi-purpose irradiation facility. ISHS Acta Horticulture 973:35-44.

USDA National Nutrient Database for Standard Reference, Release 26 (2014).

Weiss, J. and F.X. Rizzo. 1970. Cobalt-60 dosimetry in radiation research and processing. In: *Manual on Radiation Dosimetry*, eds. N.W. Holm and R.J. Berry, New York: Marcel Dekker.

Zadernowski, R., S. Czaplicki, and M. Naczk. 2009. Phenolic acid profiles of mangosteen fruits, Food Chemistry 112:685-689.